

Evaluating the Effectiveness of Skin Detection Algorithms

Habiba Mostafa 1070307, Daniela Aldave-Garza 1069571

Abstract

Skin detection is widely used in varying domains such as biometric face recognition and medical technology. It entails the recognition of skin-coloured pixels and regions in a given image. This paper presents four skin detection algorithms and analyzes their effectiveness against a baseline ground truth dataset and a relative error estimation metric. Results demonstrating how well these algorithms perform for different skin tones are provided. The performance analysis of skin detection algorithms is also supported, along with comparisons between all four algorithms to evaluate their skin detection effectiveness.

Keywords: *skin detection, face detection, skin colour, colour models, skin classification*

1. Introduction

Skin detection is the process by which skin-coloured pixels - or regions - within an image or a video are identified. It is often used as a means to detect regions of an image with potential human faces and limbs [5]. Therefore, skin detection is a fundamental operation in digital image processing and computer vision. It has implications in biometric applications such as face recognition, video surveillance and face image retrieval systems. Most research in this field has focused on identifying skin pixels in reference to colour spaces such as RGB, HSV and YCbCr.

The process of detecting skin can be complex given the varying factors that affect the overall appearance of an image. Illumination, contrast, brightness, saturation and shadows can represent colour pixels inaccurately, which introduces false positives to algorithms that are sensitive to change in illumination conditions [5]. Hence, algorithms dependent on different colour spaces have varying performances when it comes to their effectiveness at skin detection. Additionally, the presence of skin-tone coloured objects in images increases the chances of inaccuracy and false positives, given the algorithmic dependency on pixel values. This can be optimized by introducing deep learning and artificial intelligence approaches to such algorithms, resulting in enhanced skin region detection and classification outcomes.

2. Metrics

The metric used to evaluate skin segmentation algorithms investigated throughout this paper consists of a comparison of the sum of skin pixels found in the ground truth image against the sum of skin pixels detected by each algorithm in the corresponding test image. The difference between the two values represents how well an algorithm has performed. Additionally, the relative error of skin pixels measured in the resulting images is used to compare the effectiveness of the algorithms to each other. The relative error is calculated as such:

$$\text{Relative Error} = \left| \frac{v_{gt} - v_a}{v_{gt}} \right| \cdot 100$$

v_{gt} = number of skin pixels in ground truth image

v_a = number of skin pixels detected by the algorithm

In the ground truth images provided, non-skin pixels are rendered as white. Therefore, to calculate the sum of skin pixels within ground truth images, all pixels within the image are iterated and those with an RGB value that is not equal to (255, 255, 255) - i.e. pixels that are not white - are counted. On the other hand, processed images indicate non-skin pixels as black, in which case skin pixels found in the processed images are verified for having an RGB value that is not equal to (0, 0, 0).

```
for i = 0:imageWidth
    for j = 0:imageHeight
        #check if current pixel has been identified as a skin pixel
        if not pixelMap[i,j] == (0,0,0)
            counter = counter + 1
```

Given the ground truth images provided for this paper, the metrics chosen are based on verifying skin pixels in processed images against skin pixels in the ground truth images. By calculating the relative error, it can be shown how effective an algorithm is in terms of the skin pixels is classified as skin versus how many are in the actual ground truth image. This way, we are able to compare the results of what each algorithm produced.

3. Skin Detection Algorithms

Skin detection is an essential operation in image processing. It is often extended to develop biometric face detection and face recognition systems for authentication purposes. Since skin detection is influenced by parameters such as brightness, contrast, illumination, and saturation, different algorithms handle combinations of these parameters in optimized ranges. Given that such algorithms can detect varying skin tones divergently, the following skin detection algorithms will be analyzed for their effectiveness throughout this paper and will be referred to as algorithms 1, 2, 3, and 4 respectively.

3.1 Algorithm 1 - Proposed by Peter Peer

This skin detection algorithm [3] operates in the RGB colour space. A pixel in the image is classified as skin if it passes the following three conditions:

R1: $R > 95$ and $G > 40$ and $B > 20$
R2: $\max(R,G,B) - \min(R,G,B) > 15$
R3: $|R-G| > 15$ and $R > G$ and $R > B$

where R,G,B are the red, green and blue values of the pixels respectively.

```
for i = 0:imageWidth
    for j = 0:imageHeight
        r = (red value)
        g = (green value)
        b = (blue value)

        if not ((r > 95 and g > 40 and b > 20)
            and (max(r,g,b) - min(r,g,b) > 15)
            and (abs(r-g) > 15) and (r > g and r > b)):
            change pixel (row i, column j) to black
```

3.2 Algorithm 2 - Proposed by Douglas Chai

This skin detection algorithm [4] operates in the YCbCr colour space. A pixel in the image is classified as skin if it passes the following conditions:

$$R1: 77 \leq Cb \leq 127$$

$$R2: 133 \leq Cr \leq 173$$

where Cb and Cr are the Cb and Cr values of the pixel.

```
for i=0:imageWidth:
    for j = 0:imageHeight
        cb = (Cb value)
        cr = (Cr value)
        if not ((77 < cb and cb < 127) and (133 < cr and cr < 173)):
            change pixel (row i, column j) to black
```

3.3 Algorithm 3 - Skin Colour Thresholding

This skin detection algorithm references OpenCV's cv2 library to identify skin pixels within a provided image. First, it defines maximum and minimum boundaries for pixel intensities to be classified as skin pixels upon image processing. Next, it converts the input image from BGR colour space to YCbCr colour space to facilitate mask creation. To identify the skin area within the converted image, cv2's built-in method `inRange` processes the YCR image against the predefined minimum and maximum ranges and outputs a mask of the skin area detected. White pixels within the mask represent areas of the image frame that are skin. Finally, the skin mask is applied to the frame, and the processed image - with identified skin pixels - is output by the algorithm.

3.4 Algorithm 4 - RGB-H-CbCr Skin Colour Segmentation

The RGB-H-CbCr Skin Colour Segmentation skin detection algorithm [1] is based on skin tone thresholds (RGB-YCrCb). It converts the BGR image to YCbCr and HSV colour spaces then runs the RGB_H_CbCr bounding rule on all three frames. It then masks out the skin pixels detected to make up the segmented image presenting all identified skin pixels. This algorithm is often extended into face recognition detection algorithms.

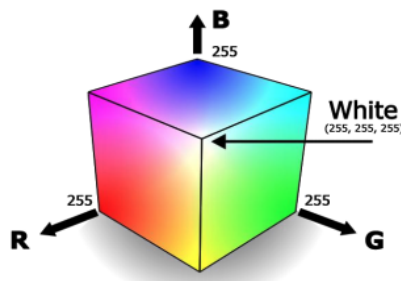


Fig. 1. RGB Colour Model [3]

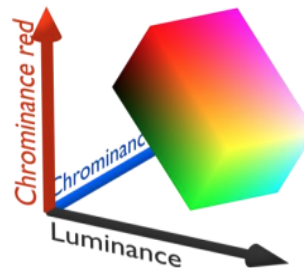


Fig. 2. CbCr Colour Model [3]

4. Experiments and Results

4.1 Test Images and Analysis

In the following experiments, each original test image (a) was processed by the four different skin detection algorithms described in Section 3. Given the sum of skin pixels as the evaluation metric adopted throughout this experiment, the total number of skin pixels per processed image was computed to evaluate the effectiveness of each algorithm. The skin pixels count of each processed image was compared against the sum of skin pixels of its ground truth image. Similarly, a comparison between all four algorithms was conducted to evaluate their overall effectiveness at skin detection.

To evaluate the effectiveness of skin detection algorithms accurately, a diverse dataset was selected to ensure sufficient coverage of varying skin tones, with respect to different races. This study was limited to referencing the provided dataset of ground truth images, hence for future implications, its accuracy can be enhanced by referencing a dataset that encompasses a larger scope of varying skin tones.

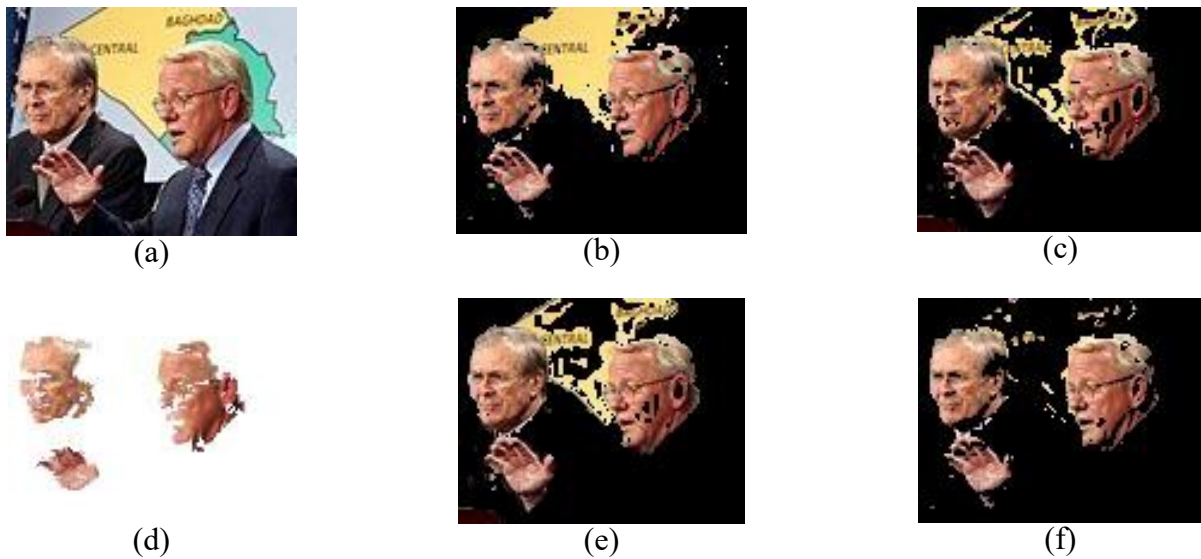


Fig. 3. Global representatives test image demonstrating processed skin pixels upon the application of four skin detection algorithms. The original image (a) has a total pixel count of 11280px, and its ground truth image (d) has a skin pixel count of 3837px. Provided is the skin detection algorithm applied to each image, followed by the sum of its identified skin pixels respectively (algorithm; sum of skin pixels): (b) algorithm1; 7149px (c) algorithm2; 7631px (e) algorithm3; 7447px (f) algorithm4; 6609px

Algorithm 4 (f) has done the best skin segmentation, visibly showing the least false positive skin pixels compared to all other algorithms. From a visual perspective, algorithms 2 (c) and 3 (e) would come in the next ranked places for their better attempt to block most of the yellow background, no more behind algorithm 4 (f) than 1022 pixels detected as skin. All algorithms have picked up a degree of yellow from the background, though correctly masking everything else out. Despite algorithm 1 (b) showing the most non-skin background, it best captured all of the true skin pixels. All the other algorithms depict some missing skin segments within the face of the men, particularly around the areas where a sudden change in brightness occurs, such as the slight shadows in the wrinkles.

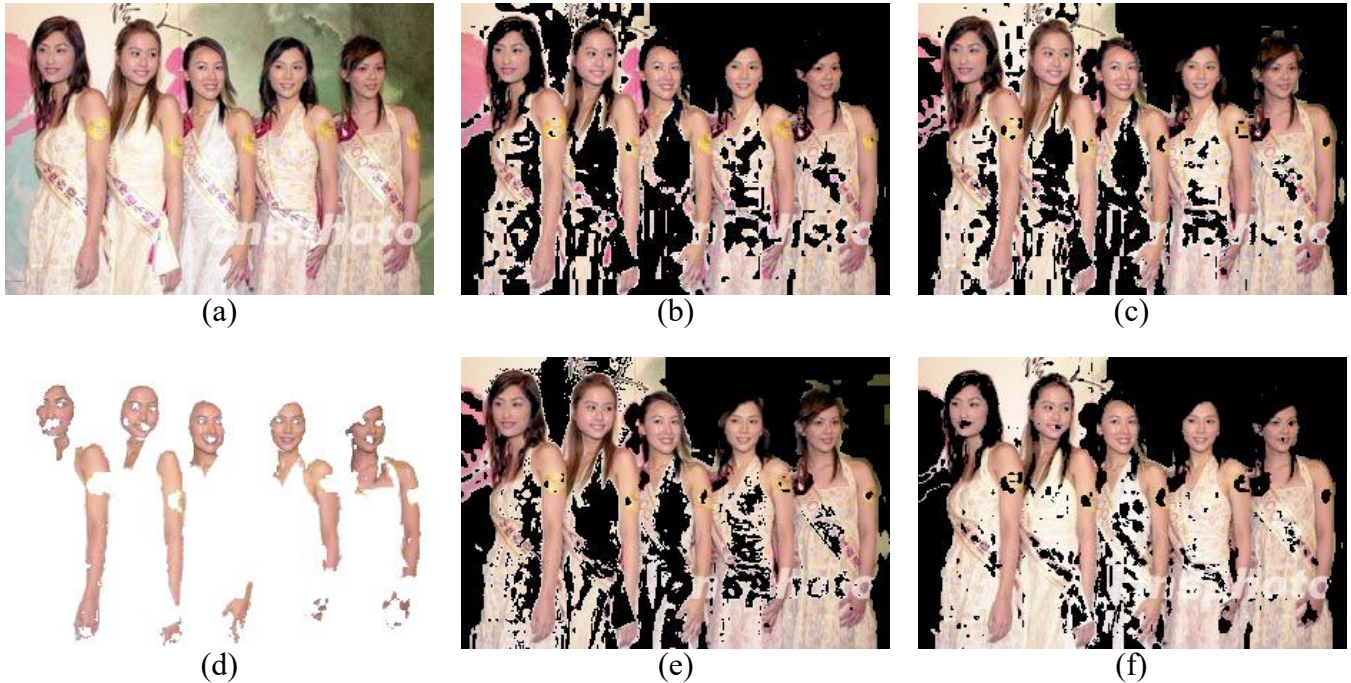


Fig. 4. Awarded models test image demonstrating processed skin pixels upon the application of four skin detection algorithms. The original image (a) has a total pixel count of 60900px, and its ground truth image (d) has a skin pixel count of 18041px. Provided is the skin detection algorithm applied to each image, followed by the sum of its identified skin pixels respectively (algorithm; sum of skin pixels): (b) algorithm1; 51564px (c) algorithm2; 53240px (e) algorithm3; 53157px (f) algorithm4; 51332px

The sections of the background and the dresses the women are wearing have a close resemblance to the colour of skin. Therefore, they have been detected as such by all algorithms, in varying degrees. According to the skin pixel count, algorithm 4 (f) produced the best results. Its resulting image has rejected the most background and hair regions, compared to all the other algorithms, while curiously retaining the most dress pixels from the original image (a). Algorithm 1 (b) comes at a close second with a difference of only 232 pixels classified as skin. It is also the algorithm that rejected the most dress pixels. In the previous test case fig. 3, it was noted that the colour yellow seems to produce false positives by most algorithms. This seems to be the case in this test as well, where parts of the pale-yellow background, the dresses worn and the pink details in the image are classified as skin.



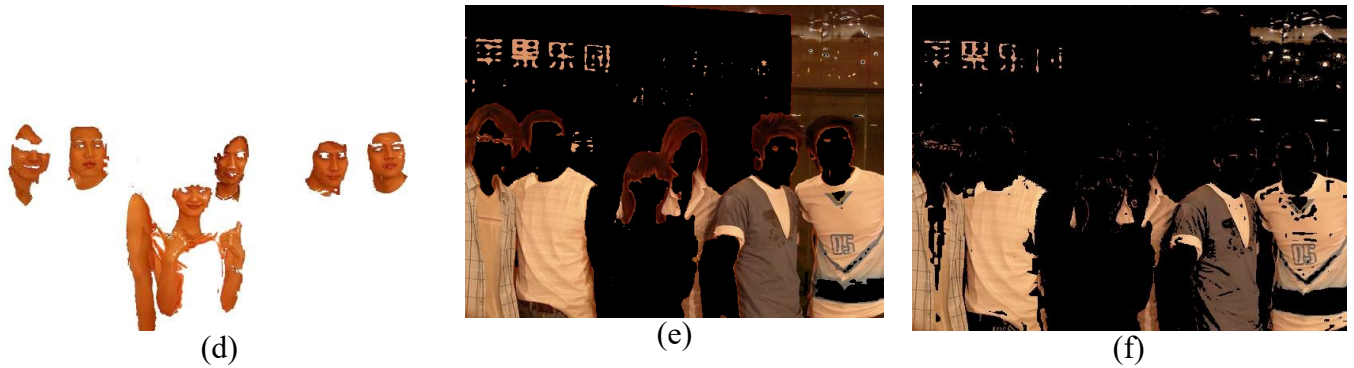


Fig. 5. Test image of a group of people demonstrating processed skin pixels upon the application of four skin detection algorithms. The original image (a) has a total pixel count of 226600px, and its ground truth image (d) has a skin pixel count of 44290px. Provided is the skin detection algorithm applied to each image, followed by the sum of its identified skin pixels respectively (algorithm; sum of skin pixels): (b) algorithm1; 188534px (c) algorithm2; 149269px (e) algorithm3; 146989px (f) algorithm4; 114801px

In the figure above, algorithms 2 (c), 3 (e), and 4 (f) have failed in the premise of skin detection, surprisingly categorizing most, if not all, of the skin pixels in the original image (a) as non-skin. The sum of classified skin pixels in algorithm 4 (f) compared to the number of skin pixels in the ground truth indicates that it is the most effective, having the lowest error in skin pixels detected (about 159% more than in the ground truth). However, it can be seen visually that it completely fails the premise of the test. Meanwhile, despite being calculated as having the greatest difference from the ground truth (about 325% more pixels classified as skin than the ground truth) algorithm 1 (b) has performed the best as it is the only one out of all algorithms tested on this image that preserved some areas of true skin. The rest of the algorithms might have failed due to the strong reddish hue throughout the image.

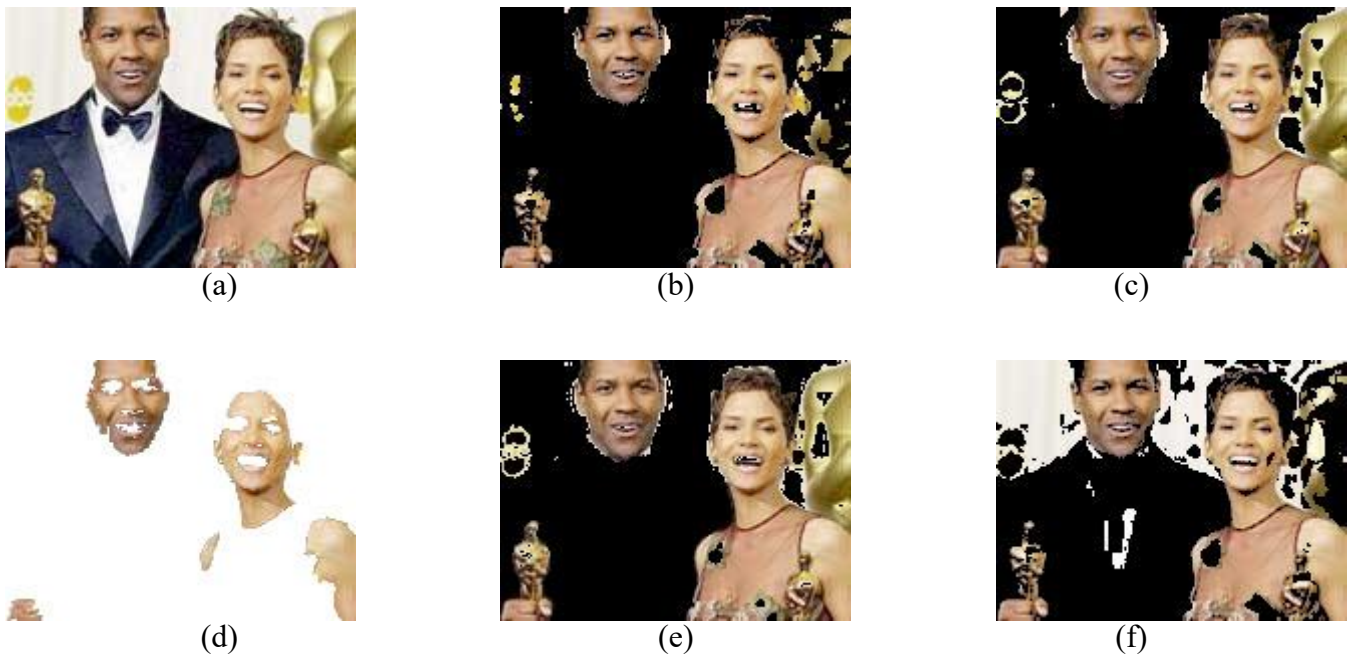


Fig. 6. Test image of awarded couple demonstrating processed skin pixels upon the application of four skin detection algorithms. The original image (a) has a total pixel count of 22750px, and its ground truth image (d) has a skin pixel count of 6498px. Provided is the skin detection algorithm applied to each image, followed by the sum of its identified skin pixels respectively (algorithm; sum of skin pixels): (b) algorithm1; 14142px (c) algorithm2; 14730px (e) algorithm3; 14688px (f) algorithm4; 16926px

All algorithms have succeeded in identifying varying tones of skin present in the image. Some other objects with similar colours to skin, such as the awards trophy and statue in the back, resulting in an increase of false positives. This may be because of the way the metal reflects in a similar way to how skin does against light. This is more apparent in the algorithms that operate in the YCbCr colour space, notably algorithms 2 (c) and 3 (e), which take brightness into account. The transparent part of the woman's dress is also a tricky section as all of the algorithms misidentified it as skin, due to it retaining a strong resemblance to other skin tones. Algorithm 1 produced the best results with the lowest in skin pixels detected compared to the ground truth, about 118% more. Next comes algorithm 3 (e) and 2 (c) a difference of 42 skin pixels detected between them. Lastly, algorithm 4 (f) exhibits the worst performance visually and with 160% more skin pixels detected than the ground truth.

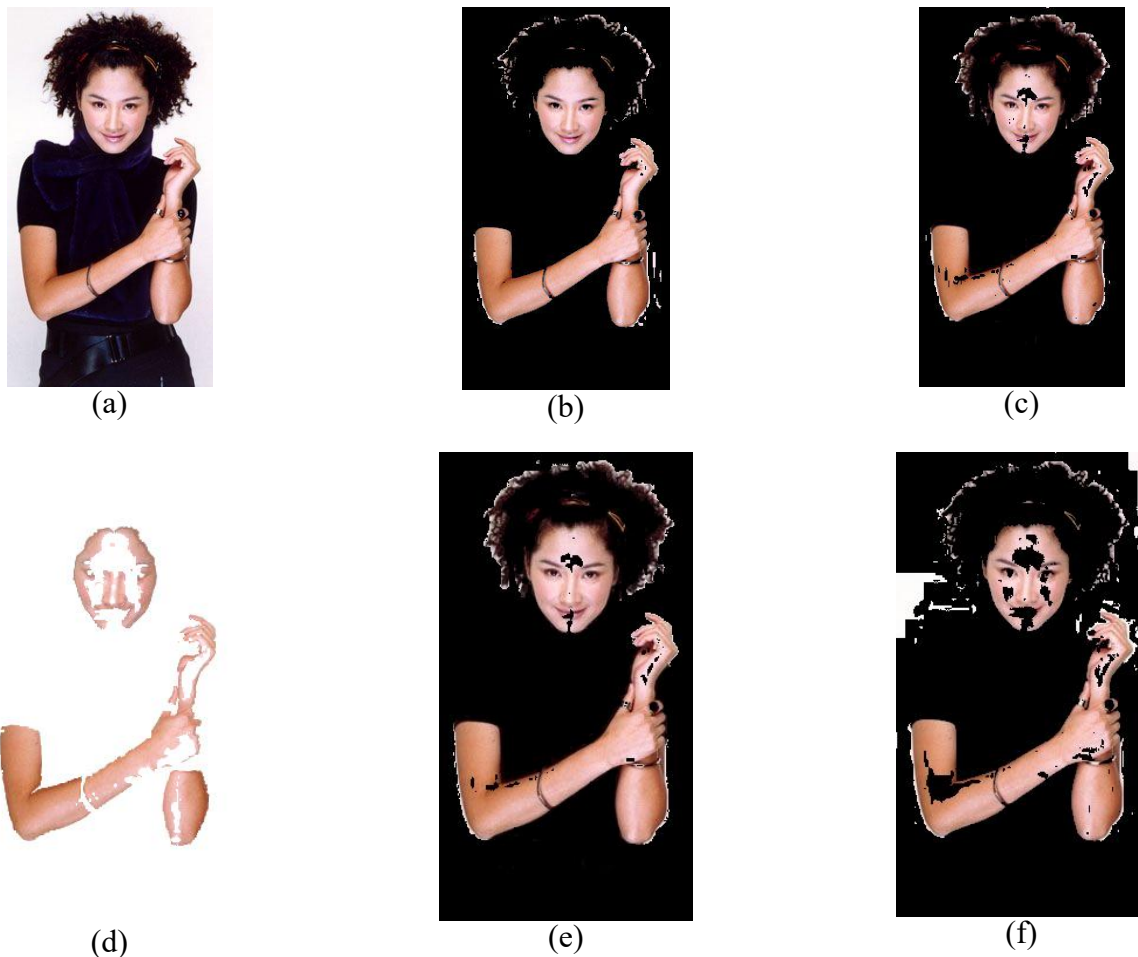


Fig. 7. Posing model test image demonstrating processed skin pixels upon the application of four skin detection algorithms. The original image (a) has a total pixel count of 86800px, and its ground truth image (d) has a skin pixel count of 16727px. Provided is the skin detection algorithm applied to each image, followed by the sum of its identified skin pixels respectively (algorithm; sum of skin pixels): (b) algorithm1; 34973px (c) algorithm2; 37717px (e) algorithm3; 37200px (f) algorithm4; 37158px

In this test, all algorithms were able to correctly distinguish between the subject and the background of the original image (a). Algorithm 1 (b) shows the best visual result of segmenting skin in the image, with minimal skin missing within established skin regions, along with having the least difference of skin pixels detected compared to the ground truth (d), about 109% more. The measured skin pixels from algorithm 4 (f) suggest that it is the second best, although it shows more false positives from the background and more missing spots of skin that were otherwise mostly detected in the other algorithms. All algorithms were able to detect the varying shades of the same skin caused by the

light and shadow in the image. It seems that the skin detection algorithms have more trouble identifying true skin pixels which are highlighted due to light, or if they are shadowed by laying on a crease of skin.

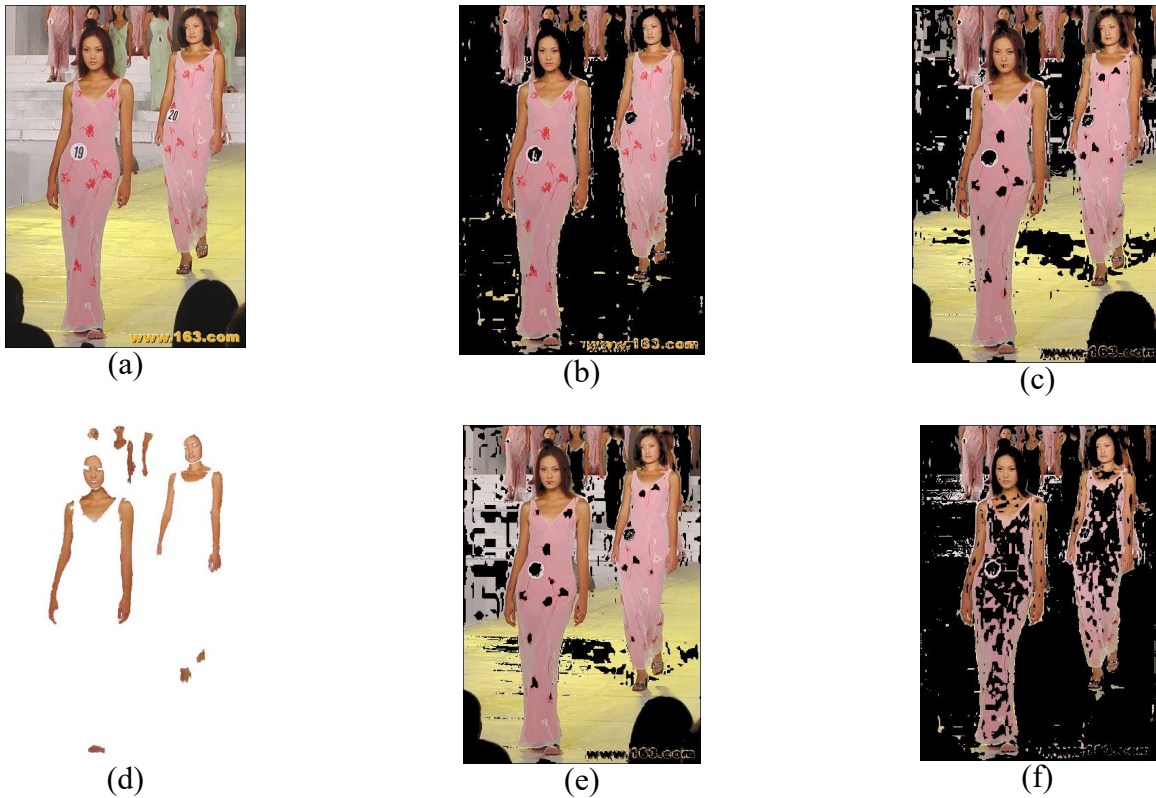


Fig. 8. Runway models test image demonstrating processed skin pixels upon the application of four skin detection algorithms. The original image (a) has a total pixel count of 175000px, and its ground truth image (d) has a skin pixel count of 24305px. Provided is the skin detection algorithm applied to each image, followed by the sum of its identified skin pixels respectively (algorithm; sum of skin pixels): (b) algorithm1; 107878px (c) algorithm2; 151541px (e) algorithm3; 162739px (f) algorithm4; 104939px

None of the algorithms were able to completely reject the pink dresses the models are wearing. The varying results may be tied to how sensitive the algorithms are to the hue as it has been observed in the previous test case Fig 2 that the colour pink tends to be classified as skin. Algorithm 4 (f) performed best in this test. It was able to classify a majority of the background as non-skin and it is the algorithm that blocked the most dress pixels. Algorithm 1 (b) showed similar visual results as algorithm 4 (f), with 2939 more pixels classified as skin. Algorithm 3 (e) had the most difficulty in this test, still retaining about 93% of the original image itself, algorithm 2 (c) fairing a little better. Once again, yellow seems to be a problematic colour that many algorithms confuse as skin.

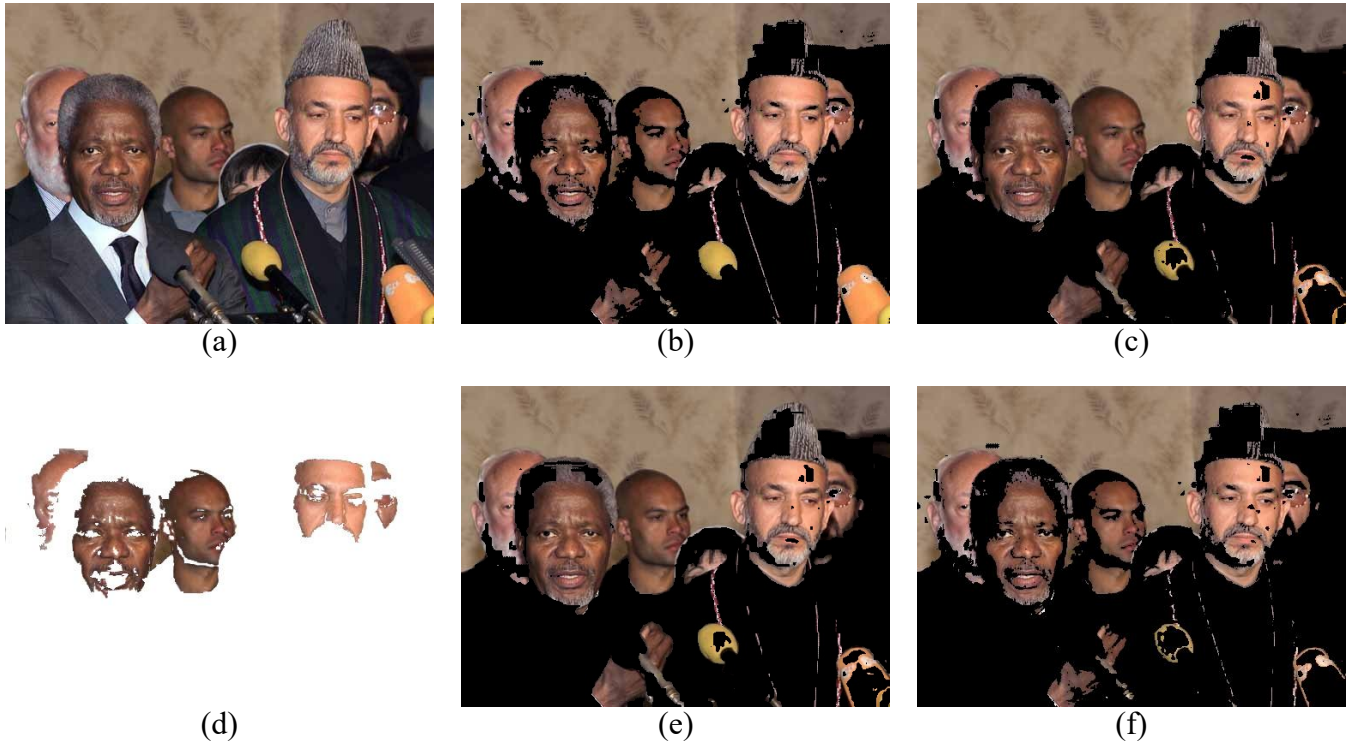
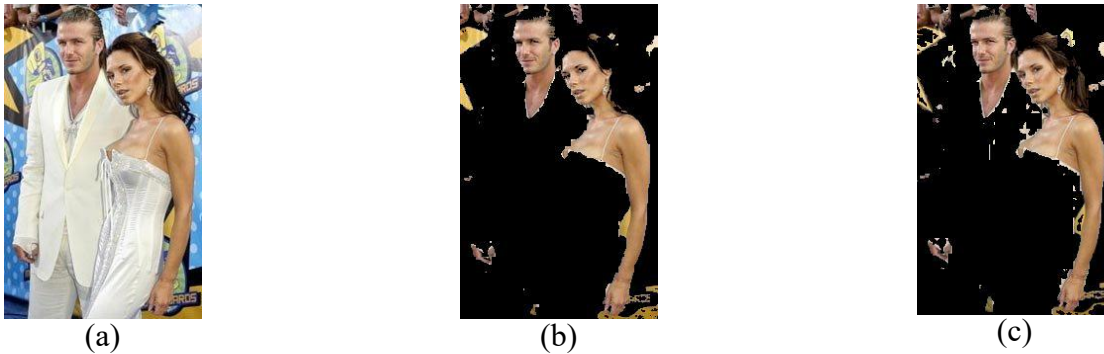


Fig. 9. Group of men test image demonstrating processed skin pixels upon the application of four skin detection algorithms. The original image (a) has a total pixel count of 187500px and its ground truth image (d) has a skin pixel count of 35575px, Provided is the skin detection algorithm applied to each image, followed by the sum of its identified skin pixels respectively (algorithm; sum of skin pixels): (b) algorithm1; 121130px (c) algorithm2; 121803px (e) algorithm3; 121925px (f) algorithm4; 113899px

Given the sensitive background of this image, which is populated with overpowering shades of nude, all four algorithms failed at classifying the surrounding pixels as non-skin pixels. With a cumulative mean skin pixel count of 119689px, compared to the ground truth (d) value of 35575px, the processed images resulted in more than 236% increase in skin pixels. Algorithm 1 (b) even identified the yellow and orange microphones as skin regions which highly indicates wide minimum/maximum RGB ranges, potentially resulting in false positives as such. On the other hand, all four algorithms succeeded at detecting all 6 faces, despite their varying skin tones. Interestingly enough, Algorithm 1 (b) identified the second last male's entire face as a skin region, while the remaining 3 algorithms identified parts of his face as non-skin, resulting in an awkward concentration of black pixels.



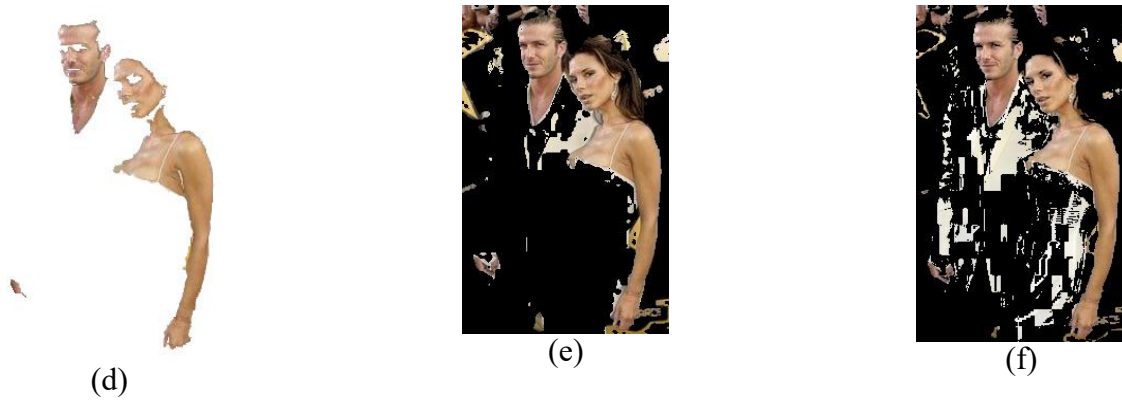


Fig. 10. Couple against graffiti wall test image demonstrating processed skin pixels upon the application of four skin detection algorithms. The original image (a) has a total pixel count of 63800px, and its ground truth image (d) has a skin pixel count of 13913px. Provided is the skin detection algorithm applied to each image, followed by the sum of its identified skin pixels respectively (algorithm; sum of skin pixels): (b) algorithm1; 26055px (c) algorithm2; 30070px (e) algorithm3; 32580px (f) algorithm4; 39267px

Though the graffiti background was handled similarly by all four algorithms, they each processed the white outfits in the original image (a) differently. Algorithm 1 (b) was the most effective at removing all non-skin pixels, having the least difference of skin pixels detected compared to the ground truth (d), about 87% more. Algorithms 2 (c) and 3 (e) came in next, with minimal difference between both. It can be observed that they both perform poorly when it comes to misidentifying hair regions in images as skin pixels. This can be due to their sensitivity to varying shades of brown, particularly in bright light intensities. Finally, algorithm 4 was of the worst performance, where it can be observed white pixels in the processed image (f) falsely identified as skin resulting in a 180% increase than the ground truth.

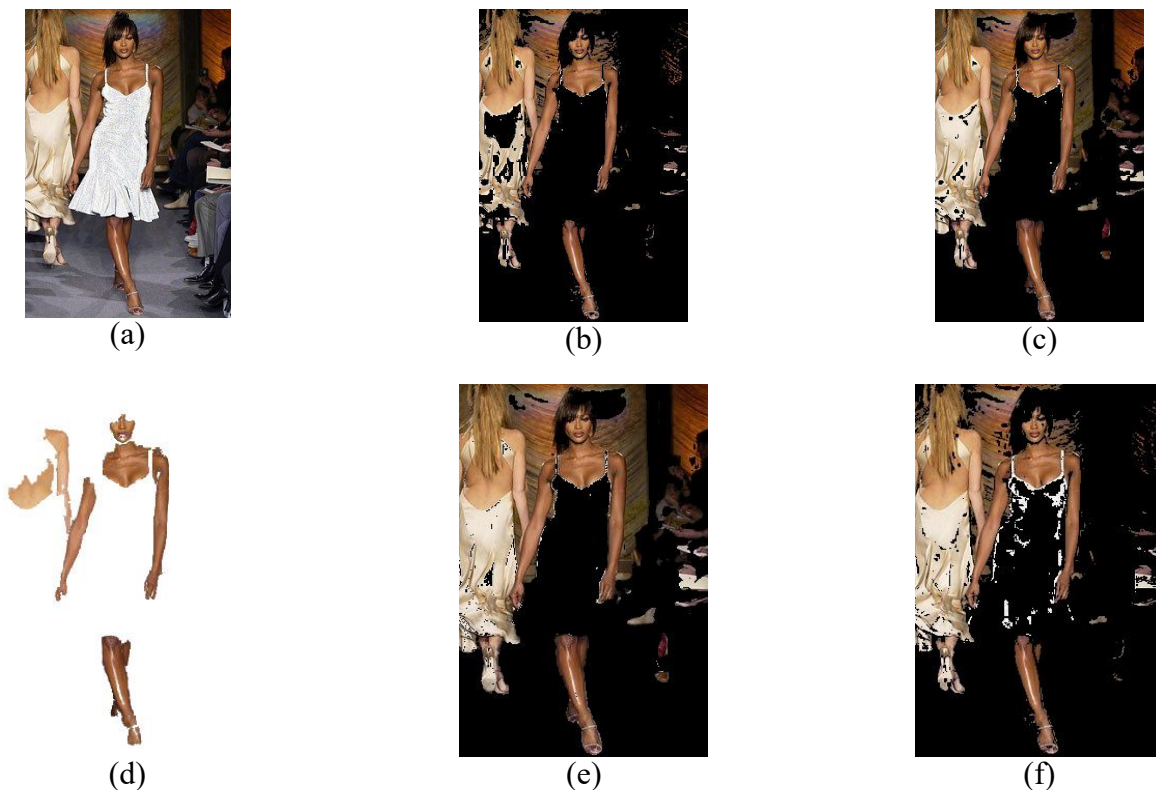


Fig. 11. Runway models test image demonstrating processed skin pixels upon the application of four skin detection algorithms. The original image (a) has a total pixel count of 86400px and its ground truth image (d) has a skin pixel count of 13337px. Provided is the skin detection algorithm applied to the image, followed by the sum of its identified skin pixels respectively (algorithm; sum of skin pixels): (b) algorithm1; 41892px (c) algorithm2; 52282px (e) algorithm3; 51795px (f) algorithm4; 43419px

Despite algorithms 1 and 4 having approximately close skin pixel values, algorithm 4 once again demonstrates limitations with processing pixels of a white tone, resulting in false negatives. However, both algorithms as observed in (b) and (f) respectively were the most effective at masking out a relative amount of the background, as opposed to algorithms 2 (c) and 3 (e), which classified most of the background as skin segmented regions. Combined, algorithms 2 and 3 on average resulted in a significant 290% increase in skin pixels, in relation to the ground truth (d) skin pixel value of 3337px. It can also be observed that all algorithms failed at masking out the second model's blonde hair, which introduces major limitations to these algorithms. This is likely due to their sole dependency on colour spaces and brightness, rather than taking texture into consideration, which can be a future enhancement to skin detection algorithm techniques. This limitation was extended to the second model's off-white dress, where all algorithms once again failed at completely detecting it as non-skin.

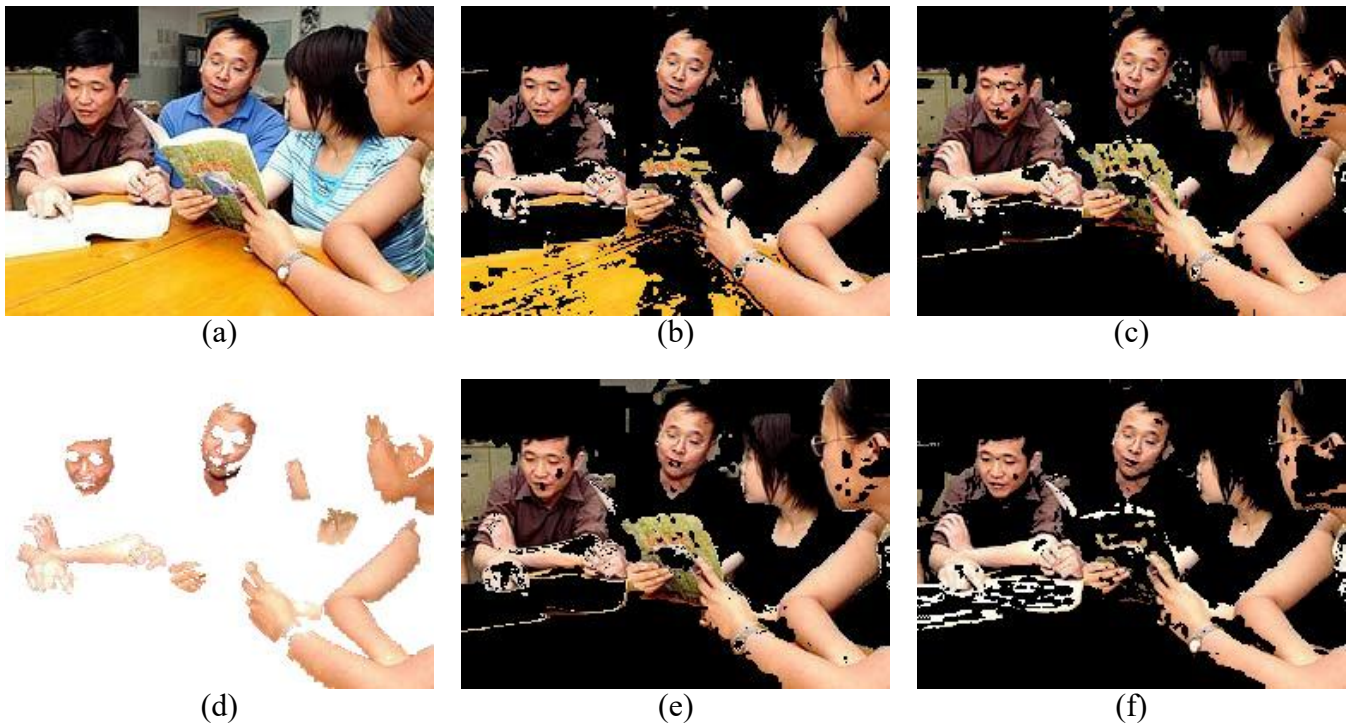


Fig. 12. Study group test image demonstrating processed skin pixels upon the application of four skin detection algorithms. The original image has a total pixel count of 45000px and its ground truth image (d) has a skin pixel count of (b) 15342px. Provided is the skin detection algorithm applied to the image, followed by the sum of its identified skin pixels respectively (algorithm; sum of skin pixels): (a) algorithm1; 34050px (c) algorithm2; 30919px (e) algorithm3; 30927px (f) algorithm4; 28086px

Though algorithm 1 (b) seems to work significantly well with identifying true positives in this image, it fails at detecting the yellow table as a non-skin region, which results in its high skin pixel value of 34050. This pattern has been observed through figures 3, 4, and 8, where the colour spaces used by some algorithms misclassify certain shades of yellow as skin. Algorithms 2 (c) and 3 (e) came in as second and third-worst, respectively. They had an almost identical count of skin pixels, with a difference of 8 pixels, though the regions identified as skin in both processed images (c) and (e) varied slightly. Finally, algorithm 4 came in first place as the best performing algorithm for this test image. Despite its observed limitations of misidentifying certain tones of white as skin pixels, its skin pixel count was 84% more than the ground truth value. Overall, aside from algorithm 1, all algorithms depict some

missing skin segments within the faces of the individuals, particularly around the areas where sudden change in brightness occurs. It can also be observed that all algorithms somewhat struggled with processing the shades of brown, identifying the majority of its instances as skin regions.

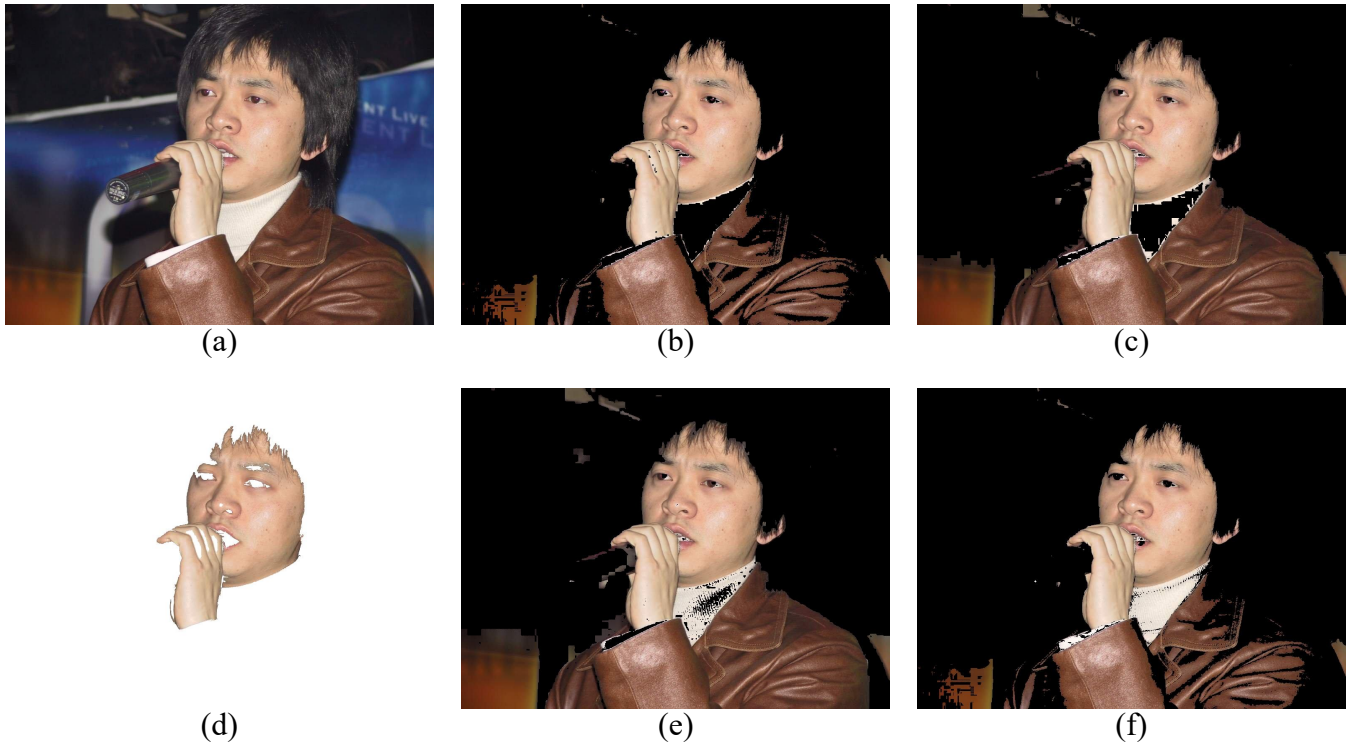


Fig. 13. Male singer test image demonstrating processed skin pixels upon the application of four skin detection algorithms. The original image (a) has a total pixel count of 786432px and its ground truth image (d) has a skin pixel count of 105004px. Provided is the skin detection algorithm applied to the image, followed by the sum of its identified skin pixels respectively (algorithm; sum of skin pixels): (b) algorithm1; 271660px (c) algorithm2; 325462px (e) algorithm3; 347277px (f) algorithm4; 280998px

All algorithms succeeded at identifying most of the background as non-skin, though parts of the warmer shades of brown towards the very top and bottom of the original image (a) were misclassified as skin pixels. More importantly, all algorithms identified the brown leather jacket as a skin region, resulting in a significant increase in false positives. This can be due to the texture of the leather, and the flashlight reflection off of it - resulting in high brightness and intense luminance. Depending on how sensitive each algorithm is to illumination, the sum of identified skin pixels varied, impacting the algorithm's overall performance. Algorithm 1 (b) seems to be the most effective in this test image, where it detected the less polished part of the leather jacket as well as the white turtleneck as non-skin, with a total 159% increase in skin pixels detected in comparison to the Ground Truth image (d). Algorithm 4 (f) had similar results, while algorithms 2 (c) and 3 (e) performed poorly with an average increase of skin pixel count by 220%.

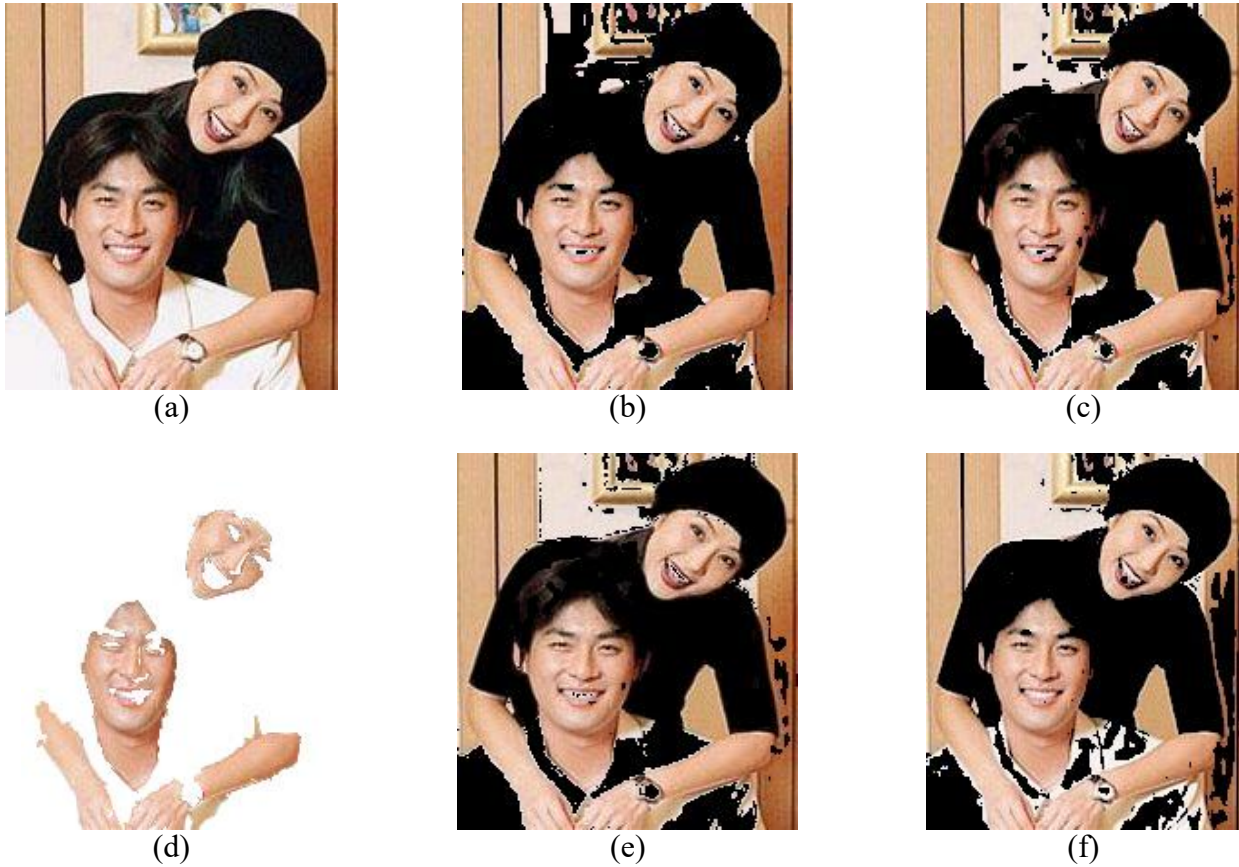


Fig. 14. Test image of two individuals demonstrating processed skin pixels upon the application of four skin detection algorithms. The original image (a) has a total pixel count of 35670px and its ground truth image (d) has a skin pixel count of 11849px. Provided is the skin detection algorithm applied to the image, followed by the sum of its identified skin pixels respectively (algorithm; sum of skin pixels): (b) algorithm1; 28359px (c) algorithm2; 31033px (e) algorithm3; 30591px (f) algorithm4; 29015px

Once again, all algorithms fail at distinguishing between the subjects and the background given its proximity to skin-tone values. Algorithm 2 (c) is the least effective at detecting skin pixels in this test, with a 162% increase in skin pixels compared to the ground truth image (d). Along with misidentifying the background as a skin region, algorithm 2 (c) and algorithm 3 (e) misidentified some of the hair regions as skin. This can be justified by their dependency on YCbCr skin colour thresholding. Additionally, from a visual perspective, it can be observed that the woman figure's arms are poorly defined. This is likely due to the male figure's shirt being white, though affected by shadow, contrast, and illumination, the white shirt has been interpreted by most algorithms to be of a light skin-tone. Algorithm 4 (f) seems to have the most challenges with misclassifying shades of white as skin pixels, which has been repeatedly observed in figures 4, 6, 10, and 11.

4.2 Overall Skin Detection Algorithms Evaluation and Analysis

<i>Skin Detection Algorithm</i>	<i>Average Relative Error of Skin Pixels Counted (across all test results)</i>
Algorithm 1	177.51992%
Algorithm 2	186.24280%
Algorithm 3	195.40975%
Algorithm 4	171.15473%

Fig. 15. Table of the four skin detection algorithms investigated throughout this paper and their computed average noise variance estimations.

Based on the Average Relative Error of skin pixels calculated across all experiments in Fig. 15, it can be concluded that given the test images referenced, algorithm 4 is most effective at segmenting skin from an image, having the lowest average of 171.15473% more pixels classified as skin than the ground truth. In second place comes algorithm 1 with an average relative error of 177.51992% of skin pixels counted in relation to the ground truth. In third place, there is algorithm 2 with an average relative error of 186.24280%. Finally, algorithm 3 is the least effective skin segmentation algorithm, having 195.40975% more pixels classified as skin than the ground truth image on average.

Throughout the test images, it has been observed that certain colours tend to be misclassified as skin by the algorithms, some more than others due to the colour spaces in which they operate. Specifically, the colour yellow, brown, white, and pink caused the most false positives among most tests. For instance, algorithm 4 demonstrated limitations with processing varying shades of white, misidentifying them as skin pixels, while algorithm 1 depicted a similar behaviour with varying shades of yellow. Across all algorithms, neutral backgrounds of skin-like tones have also been falsely identified as skin, given the algorithms' dependency on colour spaces as opposed to other factors.

It is important to note that test images of this study have been restricted to the dataset of ground truth images provided. Therefore, the evaluation metric was chosen accordingly, where ground truth skin pixels are compared against skin pixels found in the processed images, and the Average Relative Error is computed. Given restriction to the ground truth dataset provided, limitations such as:

- similarity between some images, in terms of subjects' proximity, colour of clothes, hair, background,
- an insufficiently diverse selection of skin tones,
- main use of artificial light in most images, as opposed to also investigating more instances of natural light

might have introduced some bias to the results presented throughout this paper. This can be easily enhanced by diversifying the dataset of ground truth images used, where a more inclusive selection of races, genders, subjects and background are tested and analyzed. Future enhancements to this study also include investigating skin detection algorithms that utilize convolutional neural networks, which introduces machine learning approaches to optimize the detection process and reduce false negatives.

5. Conclusion

This paper discusses different threshold-based skin detection algorithms. These algorithms are capable of processing images of different light conditions and skin tones with varying effectiveness. Results were presented and compared against all four skin detection algorithms, and against the baseline ground truth dataset. As observed, each skin detection algorithm identifies skin pixels within the test images provided based on varying criteria. The future scope of this study includes introducing elliptical structuring kernels and Gaussian blurring to the skin detection algorithms to reduce false-positive skin regions in the processed images.

References

- [1] Nusirwan bin Abdul Rahman, Kit C. Wei and John See, RGB-H-CbCr Skin Colour Model for Human Face Detection. 10.1.1.718.1964.
- [2] Saxen, Frerk & Al-Hamadi, Ayoub. (2014). colour-BASED SKIN SEGMENTATION: AN EVALUATION OF THE STATE OF THE ART. 10.13140/2.1.2103.3927.
- [3] P. Peer, F. Solina, “An Automatic Human Face Detection Method”, Proceedings of the 4th Computer Vision Winter Workshop (CVWW’99), pp. 122–130, Rastendorf, Austria, 1999.
- [4] Douglas Chai and King N. Ngan, “Face segmentation using skin colour map in videophone applications,” IEEE Transactions on Circuits and Systems for Video Technology, vol. 9, no.4, pp. 551–564, 1999.
- [5] Ahmed, E., Crystal, M., Dunxu H: “Skin Detection-a short Tutorial”, Encyclopedia of Biometrics, pp. 1218–1224 ,Springer-Verlag Berlin, Heidelberg,(2009).